ACS OMEGA

http://pubs.acs.org/journal/acsodf

Article

Flame Retardancy Behaviors of Flexible Polyurethane Foam Based on Reactive Dihydroxy P—N-containing Flame Retardants

Yulin Ding, Yumiao Su, Jiajing Huang, Ting Wang, Min-Yu Li, and Wenmu Li*

Cite This: *ACS Omega* 2021, 6, 16410−16418

Read Online

ACCESS | Metrics & More | Article Recommendations | Supporting Information

ABSTRACT: Green and environment-friendly high-efficiency flame retardants (FRs) are crucial to polymer FR modification. Here, a green FR 2-((bis(2-hydroxyethyl)amino)methyl)-5,5-dimethyl-1,3,2-dioxaphosphinane 2-oxide (HAMPP) was synthesized. The HAMPP was incorporated with a cyclic phosphorus structure, which will readily carbonize to inhibit or prevent further combustion. Moreover, the HAMPP contains dihydroxy reactive groups that can be used as a monomer in the polymerization reaction to obtain the main chain containing phosphorus polymer. Research studies on FRs were based on flexible polyurethane foam (PU-HAMPPs). The limiting oxygen index value of PU foam with 10% HAMPP could reach 23.7%, passing a UL-94 V-0 rating together. With the addition of HAMPP, the peak heat release rate of PU foam decreased significantly, the decomposition temperature increased, the heat release capacity reduced by 31%, and the char yield increased by 42%. The chemical composition and morphology of the char residual have been studied and analyzed thoroughly. We find that HAMPP forms a molten viscous protective layer uniformly on the material surface and releases some incombustible gases. These indicated that the FR exploited both condensed-phase and gas-phase flame retardancy mechanisms. Besides, the addition of FRs improved the mechanical properties.

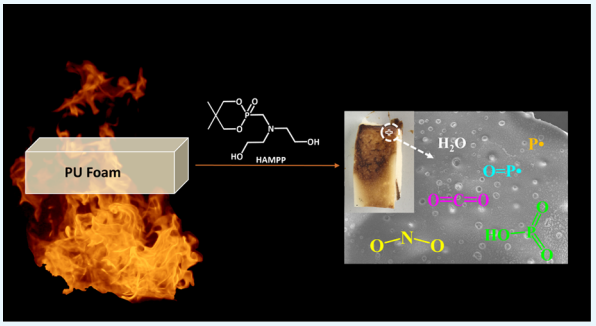

1. INTRODUCTION

Flexible polyurethane foam applications are ubiquitous in various industries: packing material, furniture cushion, soundproof material, and transportation.[1−4] This material has an inherent problem of low oxygen index, which makes it extremely flammable. Besides, this material will release a large amount of toxic smoke during the burning process, causing serious harm to humans. Hence, the development of effective flame retardants (FRs) on flexible PU foam plays a vital role in reducing fire risk and improving human life safety.[5,6]

FR based on halogen (H-FRs) had been widely used in polyurethane materials for a long time because of their highly efficient FR effect. However, studies have shown that the H-FRs produce corrosive and toxic fumes during combustion and even release cancer-causing dibenzofurans and halogenated dibenzodioxins.[7,8] At present, many countries have legislated against the use of such FRs.[9] Therefore, there is an urgent need to find alternatives to halogen FRs.

In recent years, various halogen-free FRs have been studied and developed as alternatives, such as silicon FRs, nitrogen FRs, and phosphorus FRs.[10−12] Among them, phosphorus-containing FRs (P-FRs) are particularly excellent in virtue of their chemical versatility and high-efficiency flame retardancy even at low loading,[5] which have good development prospects.[13] Liu et al. prepared P-FRs that can decompose earlier to form the char, which could isolate the transfer of heat and O_2 between the FR and material while releasing water and restraining the generation of the combustible gas.[14] However, with the development of application requirements, single phosphorus-containing FRs can no longer meet the demands of new materials or high flame retardancy. Therefore, synergistic FRs with multiple FR mechanisms have gradually become a hot spot for research.[15]

The use of P—N-containing FRs (P—N FRs) is extensively studied, and their flame retardancy in many cases attributed to the gas- and condensed-phase synergistic effects.[16−19] Therefore, P—N FR has been a principal research trend in recent years. Liu et al. studied a DOPO-based derivative DTE-DOPO, which contains many phosphorus compounds in both the gas phase and condensed phase to reduce the generation of toxic gases.[20] Yuan et al. synthesized two P—N FRs (BHPP and MADP).[21] Among O═P—O, triazine ring group and NH_3 help to form dense and continuous carbon residue.

Although many P-FRs and P−N FRs have been developed, most of them are small-molecule additive FRs, and they are

Received: March 9, 2021
Accepted: June 3, 2021
Published: June 16, 2021

Scheme 1. Synthesis Routes of DMPP, HENH, and HAMPP

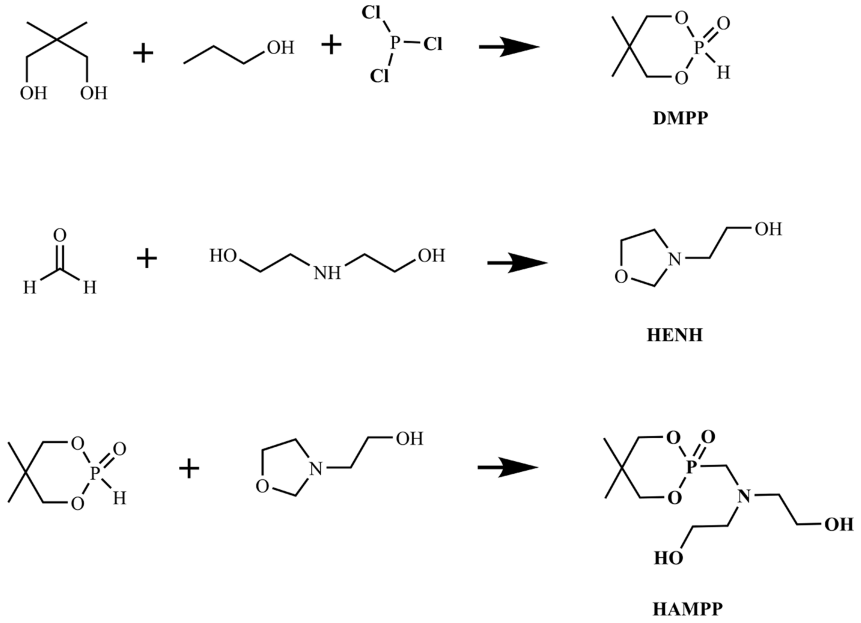

blended with materials in the small-molecule form to achieve the FR properties. However, these FRs have the following problems and shortcomings:[22−24] (1) the addition of additive FRs is prone to phase separation defects, which will undoubtedly affect the matrix polymer performance; (2) additive FRs are easy to migrate in the matrix material, resulting in unstable FR performance; and (3) phosphorus-containing small-molecule FRs also have a certain degree of toxicity and are easy to volatilize to cause environmental pollution and harm human health. Thus, it is necessary to research and investigate high-efficiency reactive P-N FRs, which are green and environmentally friendly.

Therefore, we have designed a reactive P−N FR (HAMPP) based on the above situation. This study uses a cyclic phosphorus-containing (DMPP) and nitrogen-containing five-membered ring (HENE) to synthesize HAMPP. DMPP can decompose into phosphoric acid or polyphosphate at high temperatures. It will be dehydrated and carbonized to form a molten viscous protective layer on the material surface to inhibit or prevent further combustion. HENE can decompose into incombustible gases such as water, ammonia, and nitrogen. The gases absorb lots of heat, heavily reduce the material surface temperature, and dilute the combustible gas. Meanwhile, the nitrogen-containing part can delay the oxidation and volatilization loss of the phosphorus-containing by releasing refractory gas. The dihydroxy structure can be used as a monomer in the polymerization reaction or a component in the copolymerization reaction to obtain the main chain containing phosphorus polymer. It can also be used as an oligomer and polymer to undergo a graft reaction to form a branched phosphorous polymer, which can avoid the problems faced by small-molecule FRs. A series of flexible polyurethane foam containing different FR (PU-HAMPPs) contents were prepared. The results of FR performance and thermal analysis were obtained. Because of its dihydroxy structure that can combine with the flexible polyurethane main chain through covalent bonds, this connection not only prolongs the FR timeliness but also improves the polyurethane mechanical properties.

2. EXPERIMENTAL SECTION

2.1. Materials. Phosphorus trichloride (PCl_3), ethanol, polyether polyol (3000 g/mol and a hydroxyl value of 56 mg KOH/g), and diisocyanate (average functionality of 2.7, NCO content of 30%) were supplied by Sinopharm (Shanghai, China). Toluene diisocyanate (2,4,2,6) (TDI) and polyoxymethylene were bought from Aladdin (Shanghai, China). Tin(II)2-ethylhexanoate, neopentyl glycol, and diethanolamine (DEA) were provided by Macklin (Shanghai, China). Silicone surfactant and 1,8-diazabicyclo [5,4,0]-7-undecene (>98%) were purchased from TCI (Shanghai, China).

2.2. Synthesis of 5,5-Dimethyl-1,3,2-dioxaphos-phinane 2-oxide. In a 500 mL three-necked round-bottomed glass flask, ethanol (1 mol, 31 g) and 2,2-dimethyl-1,3-propanediol (1 mol, 104.15 g) were mixed and stirred, while phosphorus (1 mol, 137.34 g) trichloride was added dropwise. The reaction temperature shall not be higher than 25 °C until the dropwise addition of phosphorus oxychloride had completed and the exothermic reaction had got over. After that, the mixture was stirred at 25 °C while nitrogen was passed through to remove the liberated hydrogen chloride and ethyl chloride. Then the temperature of the mixture was raised to 100 °C to remove the byproducts completely. Finally, a white, crystalline solid was distilled at 140−145 °C through a short Vigreux column.[25] ^{1}H NMR (400 MHz, DMSO-d_6): 7.75 (s, 1H), 6.06 (s, 1H), 4.25 (s, 4H), 3.91 (d, J = 33.4 Hz, 4H), 1.16 (s, 6H), 0.81 (s, 6H). ^{31}P NMR (162 MHz, DMSO-d_6): −7.92 (p, J = 12.0 Hz).

2.3. Synthesis of 2-(Oxazolidin-3-yl)ethan-1-ol (HENH). DEA (1 mol, 105.14 g) was warmed to 45 °C under a nitrogen gas atmosphere, and then, paraformaldehyde (1 mol, 30 g) was added slowly upon stirring. After paraformaldehyde had been added, the colorless liquid was presented, keeping the reaction for 2 h. Then, the temperature was raised to 80 °C, and evaporated water was removed by vacuum distillation for 2 h. Faint yellow viscous liquid was obtained in the flask. ^{1}H NMR (400 MHz, DMSO-d_6): 4.54−4.47 (m, 1H), 4.15 (s, 2H), 3.60 (t, J = 6.7 Hz, 2H), 3.52−3.44

https://doi.org/10.1021/acsomega.1c01267
ACS Omega 2021, 6, 16410−16418

(m, 2H), 2.87 (t, J = 6.7 Hz, 2H), 2.53 (dd, J = 13.7, 7.5 Hz, 2H).

2.4. Synthesis of 2-((Bis(2-hydroxyethyl) amino) methyl)-5,5-dimethyl-1,3,2-dioxaphosphinane 2-oxide (HAMPP). HENH (1 mol, 117.15 g) and 2.2 g of catalyst for macroporous acid resin (D001) were mixed and stirred at 50 °C under nitrogen atmosphere, and then, DMPP (1 mol, 150 g) was added slowly. After the addition of DMPP is completed, this reaction is kept for 2 h. A brown transparent viscous liquid was achieved.^{1}H NMR (400 MHz, DMSO-d_6): 4.46 (s, 1H), 4.15 (dt, J = 10.8, 5.6 Hz, 2H), 3.91 (dd, J = 15.9, 10.8 Hz, 1H), 3.48 (h, J = 5.8 Hz, 4H), 3.24−3.13 (m, 2H), 2.70 (t, J = 6.2 Hz, 3H), 1.09 (s, 2H), 0.86 (d, J = 13.7 Hz, 3H). ^{31}P NMR (162 MHz, DMSO-d_6): 17.39.

The synthesis routes of DMPP, HENH, and HAMPP are shown in Scheme 1.

2.5. FR of Polyurethane Foam (PU-HAMPPs). Except for TDI and diisocyanate, all ingredients were mixed and stirred well first. TDI and diisocyanate have subsequently added the former mixture and mechanical stirring for the 30 s. At last, this mixture was cured at 120 °C for 20 min. The composition of all PU-HAMPP samples are listed in Table 1. All samples are synthesized in the same way.

Table 1. Composition, LOI, and UL-94 of Pure PU and PU-HAMPP Samples

samples	PU foam (wt %)	HAMPP content (wt %)	LOI (%)	UL-94
pure PU	100	0	19	V-2
PU-5	95	5	20.2	V-2
PU-8	92	8	23.2	V-2
PU-10	90	10	23.7	V-0

The synthesis route of PU-HAMPP is shown in Scheme 2.

2.6. Characterization. All nuclear magnetic resonance (NMR) measurements were obtained on AVANCE 400 Bruker spectrometer (DMSO-d_6 as solvent). Fourier transforms infrared (FTIR) spectra were performed by VERTEX 70, Bruker (Germany). The mass spectra (MS) was conducted by impact (Germany). The limiting oxygen index (LOI) values used a JF-3 oxygen index meter (China). The UL-94 vertical burning test used the CZF-5CD 50W vertical burning instrument (China). The thermogravimetric analysis (TGA) of samples was performed on a NETZSCH STA449F3 thermal analyzer from 30 to 700 °C under a nitrogen atmosphere with a heating rate of 20 K/min. Microscale combustion calorimeter (MCC) test was conducted by using FAA Micro Calorimeter. The Zeiss Sigma 300 SEM was used to observe scanning electron microscope (SEM) images. The scalable 250xi Thermo Fisher Scientific was used to record the X-ray photoelectron spectroscopy (XPS) of char residue. All physical property measurements were measured on AG-X plus 100KN (SHIMADZU) Universal Material Testing Machine. The size of stretching properties of specimens was 4 × 10 × 40 mm. The size of compressive properties of specimens was 10 × 10 × 10 mm.

3. RESULTS AND DISCUSSION

3.1. Structure of FRs. ^{1}H NMR spectrum confirms the structure of DMPP, as shown in Figure S1. The peaks at 7.75 and 6.06 ppm belong to the P−H. The peaks at 4.25 and 3.87 ppm are assigned to O−CH_2. In the ^{31}P NMR spectrum, as shown in Figure S2, the single peak at −7.02 ppm further verifies the purity of the compound.[26] Figure 1 shows the ^{1}H

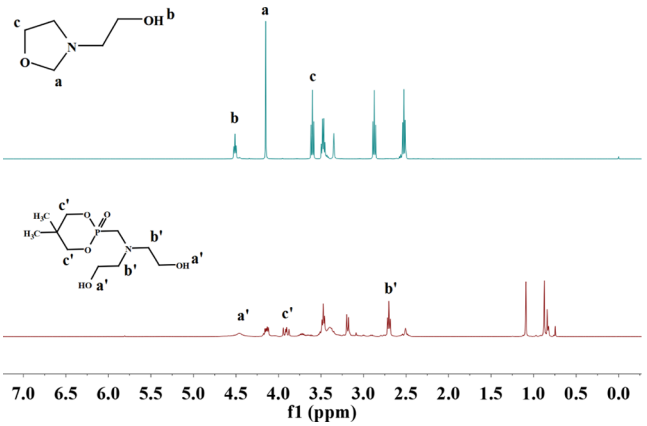

Figure 1. ^{1}H NMR of HENH and HAMPP.

NMR spectrum comparison of HENH and HAMPP. The peak at 4.51 ppm is ascribed to the C−OH. The chemical peak at 4.15 ppm is attributed to N−CH_2−O groups. The peak at 3.60 ppm is associated with O−CH_2. The peak at 2.70 ppm is attributed to N−CH_2. Figure S3 reveals the signal shift of the ^{31}P NMR spectrum at −17.44 ppm. These combined analyses prove the successful preparation of HAMPP (shown in Figures S4 and S5).

The MS can further investigate the sequence structure of the HAMPP presented in Figure 2. The peak at 290 m/z corresponds to $C_{10}H_{22}NNaO_5P$ and the peak at 557 m/z is its dioligomer.

Figure 3 shows the FTIR of materials. For the PFR, the characteristic peaks at 817 and 1008 cm^{-1} are attributed to the P—O—C. The stretching vibration at 1223 cm^{-1} is ascribed to the P═O groups, the peaks at 2870 and 2950 cm^{-1} belong to the stretching absorption peaks in saturated CH_2, and the characteristic peak at 3360 cm^{-1} is allocated to the absorption band of —OH.

Compared with PU-10 curves, we can see in the PU-10 that the peak at 3360 cm^{-1} has disappeared, while the new peak at

Scheme 2. Synthesis Route of PU-HAMPP

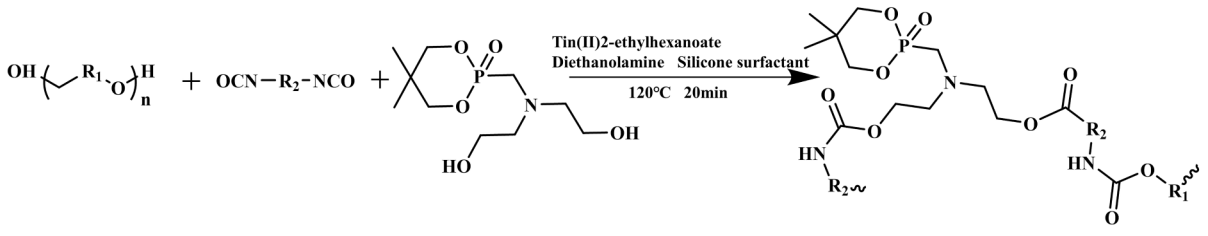

https://doi.org/10.1021/acsomega.1c01267
ACS Omega 2021, 6, 16410−16418

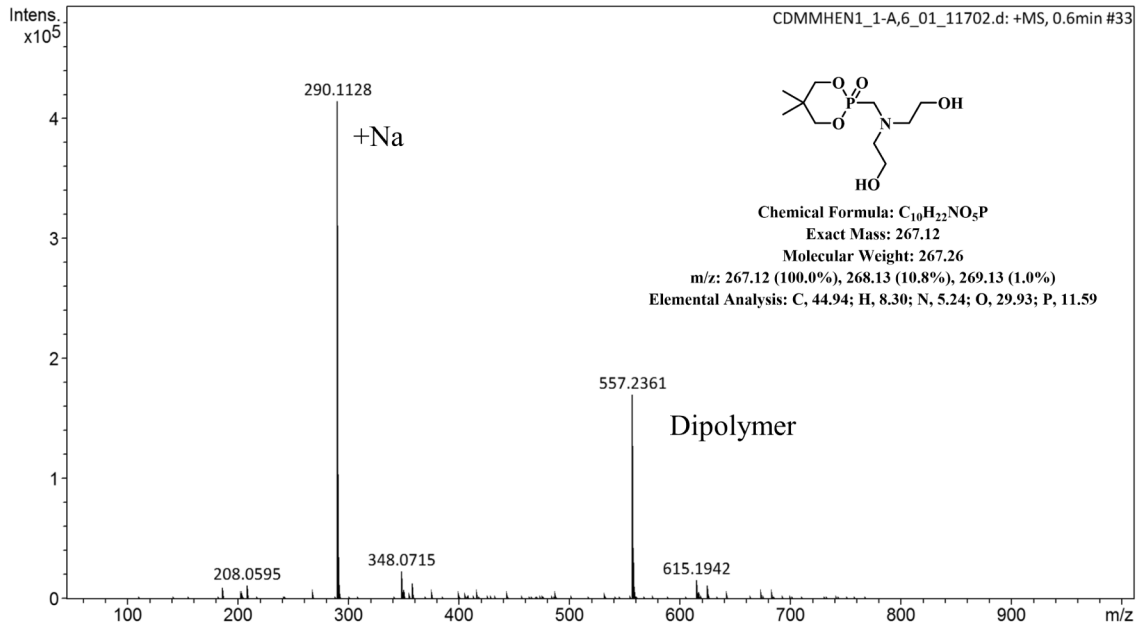

Figure 2. MS spectrum of HAMPP.

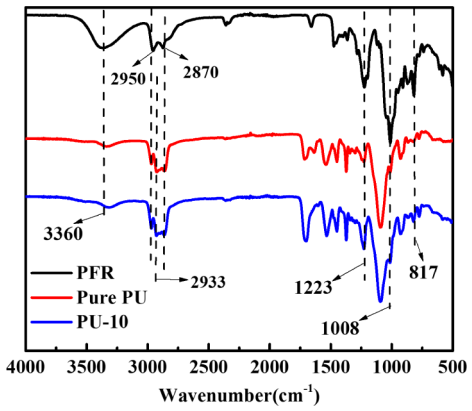

Figure 3. FTIR of HAMPP, pure PU, and PU-10.

2933 cm^{-1} is assigned to the C−H stretching vibration in the methyl and methylene group of carbamates.

On comparing the curves of pure PU and PU-10 and the peaks of P−O−C at 817 and 1008 cm^{-1}, the characteristic peak of PFR appears on the PU-10 curves. The dihydroxy functional group in the HAMPP reacts with the NCO group in the isocyanate to form carbamates. This reaction can connect the FR into the molecular chain of the matrix material to avoid the problem of easy migration of the added small-molecule FR and short FR timeliness.

These details mean the successful synthesis of PU-HAMPP.[27]

3.2. LOI, UL-94, and Thermal Property Tests. The LOI values and UL-94 rating appear in Table 1. The flame retardancy of pure PU and PU-HAMPPs is assessed by LOI values and UL-94 tests. With the increase in HAMPP, the LOI value rises from 19% to 23.7% and the PU-10 exhibits the highest. Furthermore, the UL-94 rating of PU-10 was improved to V-0 rating, which presents the combustion rate of materials. The result indicates that HAMPP works well in flame-retarding flexible PU foam.

Polyurethane has a low oxygen index and easy to drip during burning. Therefore, it is difficult for this material to reach the V-0 grade of UL-94. We added phosphorus- and nitrogen-containing FR, though the condensed-phase and gas-phase FR mechanisms were applied to reduce the material flammability to achieve the V-0 grade. From SEM images, we can see that the PU-5 and PU-8 do not form uniform cells and dense carbon layers, while PU-10 contains the above two simultaneously. Therefore, PU-10 has reached a good UL-94 test level. Figure S6 shows the carbon layer photo of FR PU foams.

The MCC is a universal method for studying thermal stability property analysis. The MCC data of the samples are shown in Table 2. From tabulation, the peak heat release rate (PHRR) of pure PU is 346.5 w/g, while the PHRR of PU-5 decreases 31% down to 238 w/g. Although the heat release of PU-HAMPPs shows an upward trend with the increased content of HAMPP, the total amount is lower than that of pure PU.

Table 2. MCC Data for Pure PU and PU-HAMPPs

samples	HR capacity (J g^{-1} K^{-1})	PHRR (w/g)	THR (kJ/g)	temperature (°C)
pure PU	345	346.5	20.4	409.7
PU-5	238	239.0	13.3	425.7
PU-8	299	299.7	16.8	415.5
PU-10	301	299.6	16.0	414.4

The PHRR values of the materials are all around 400 °C. At this temperature, the mass loss of the FR has exceeded 70% by TG curves. Thus, we can see the thermal decomposition of FRs is an exothermic process. PU-5 has the lowest PHRR because of the lowest addition of HAMPP. With the increase in the added FR, the heat released of HAMPP will increase. This is why PU-5 has the lowest PHRR, while PU-10 has the highest PHRR.

Figure 4 shows two HRR peaks, and the curves of PU-HAMPPs are lower than those of the pure PU. The result confirms that with the addition of HAMPP, the PHRR shifts

https://doi.org/10.1021/acsomega.1c01267
ACS Omega 2021, 6, 16410−16418

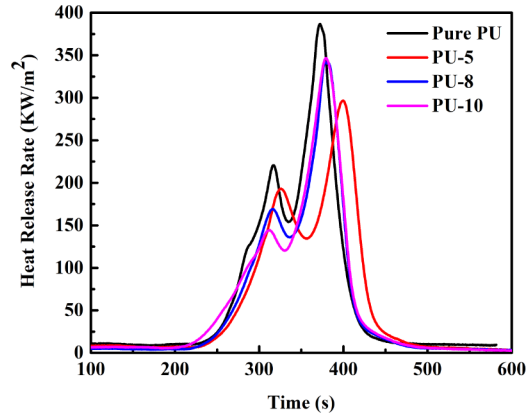

Figure 4. HRR curves of pure PU and PU-HAMPP foams.

move backward, indicating that the FR protects the PU foam by reducing heat released during the combustion process.

Figure 5 shows the TG and DTG curves in nitrogen. The temperature at 5% mass loss ($T_{-5\%}$). Table 3 lists the maximum mass loss (T_{max}) and the char residue (%) at 700 °C. The $T_{-5\%}$ of PU-HAMPPs shows a significant downward trend with the gradual increase in the amount of FR, which may be due to the O═P—O bond in HAMPP that is prone to break than the C—C,[7] which corresponded to the test results of MCC. The char yield at 700 °C for PU-10 is 4.7%, which is 42% higher than that for pure PU. The reduction of T_{max} ascribes to the decomposing of HAMPP and the formation of polyphosphate. Compared with pure PU, PU-HAMPPs have a lower temperature of initial decomposition. The incorporation of HAMPP can improve the material stability at high temperatures and promote char residue formation.

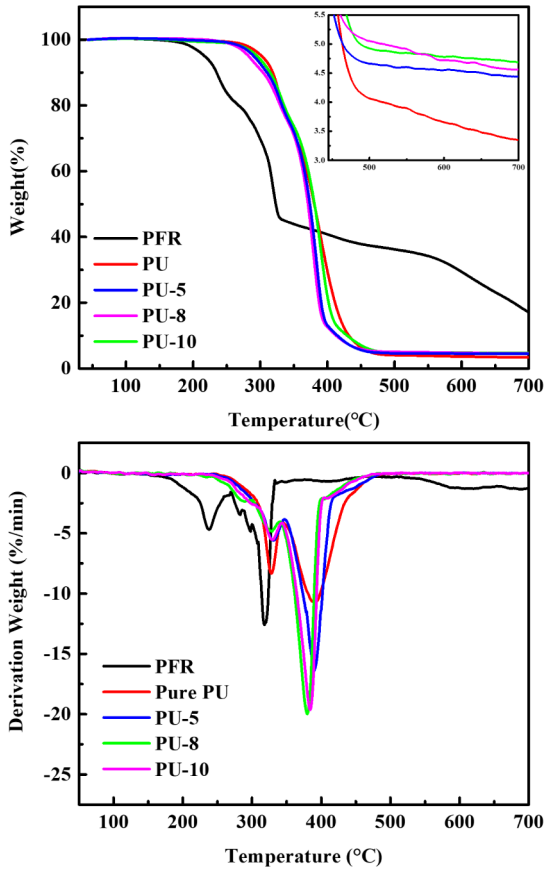

Figure 5. (a) TG and (b) DTG curves of HAMPP and pure PU, PU-5, PU-8, and PU-10 in a nitrogen atmosphere.

Table 3. TG Data of HAMPP, Pure PU, and PU-HAMPP Hybrids in Nitrogen

samples	$T_{-5\%}$ (°C)	T_{max} (°C)	char residue (%) at 700 °C
PFR	217.2	237.4, 319.6	10.52
pure PU	302.3	328.9, 391.0	3.3
PU-5	295.4	328.2, 389.4	4.4
PU-8	290.3	329.6, 384.8	4.6
PU-10	282.6	289.3, 328.5, 380.5	4.7

The TG and DTG curves of PFR, PU-5, PU-8, and PU-10 in the air atmosphere are shown in Figure 6, and the data are

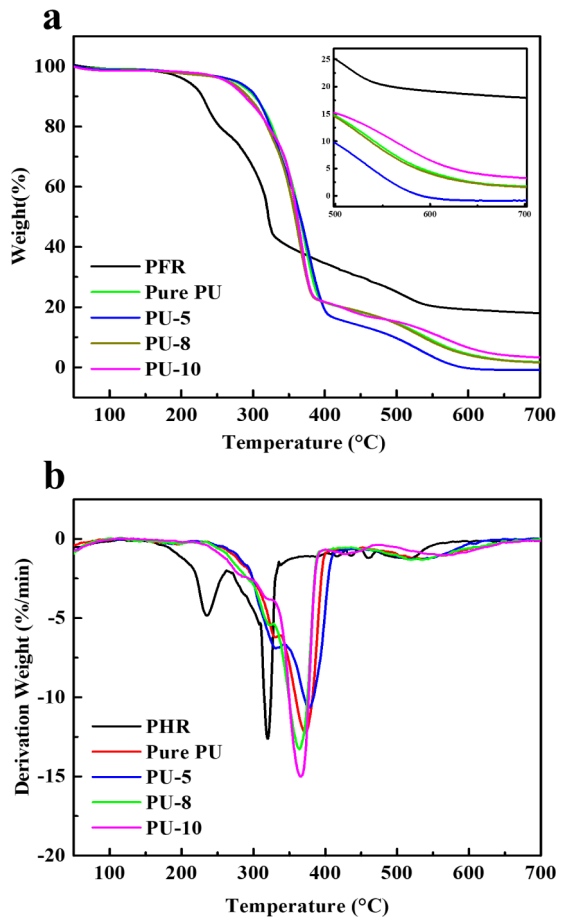

Figure 6. (c) TG and (d) DTG curves of HAMPP and pure PU, PU-5, PU-8, and PU-10 in air atmosphere.

Table 4. TG Data of HAMPP, Pure PU, and PU-HAMPP Hybrids in Air

samples	$T_{-5\%}$ (°C)	T_{max} (°C)	char residue (%) at 700 °C
PFR	208.7	235.4, 320.3	18.29
pure PU	277	335.4, 377.6	0
PU-5	273.9	330.4, 371.3	1.9
PU-8	265.7	319.7, 364.8	1.5
PU-10	262.9	319.3, 367.0	2.3

https://doi.org/10.1021/acsomega.1c01267
ACS Omega 2021, 6, 16410−16418

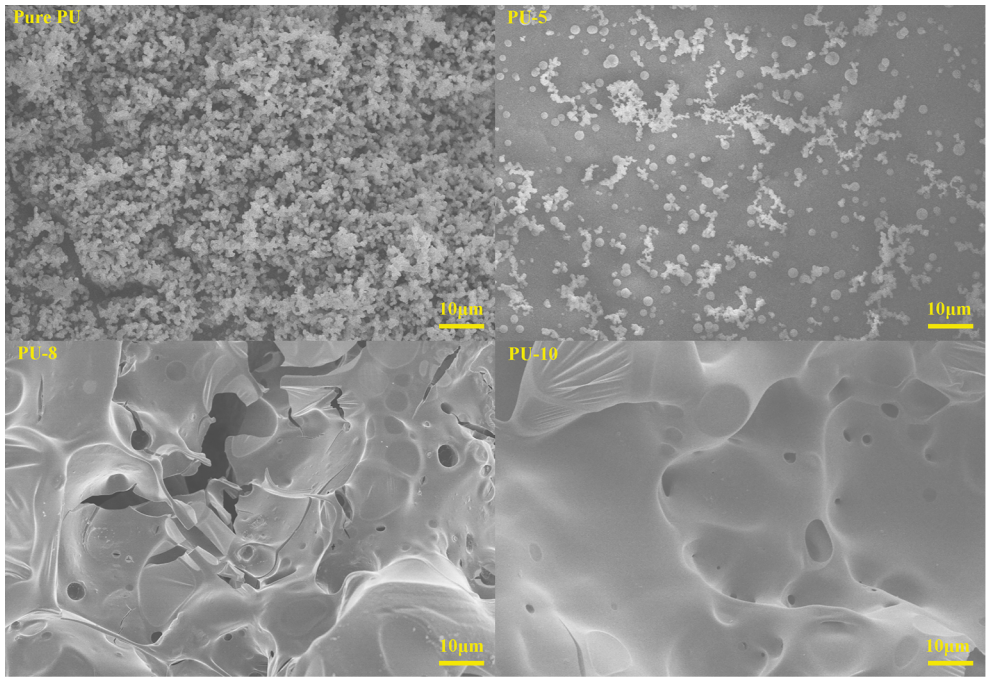

Figure 7. SEM photographs of pure PU, PU-5, PU-8, and PU-10 foam.

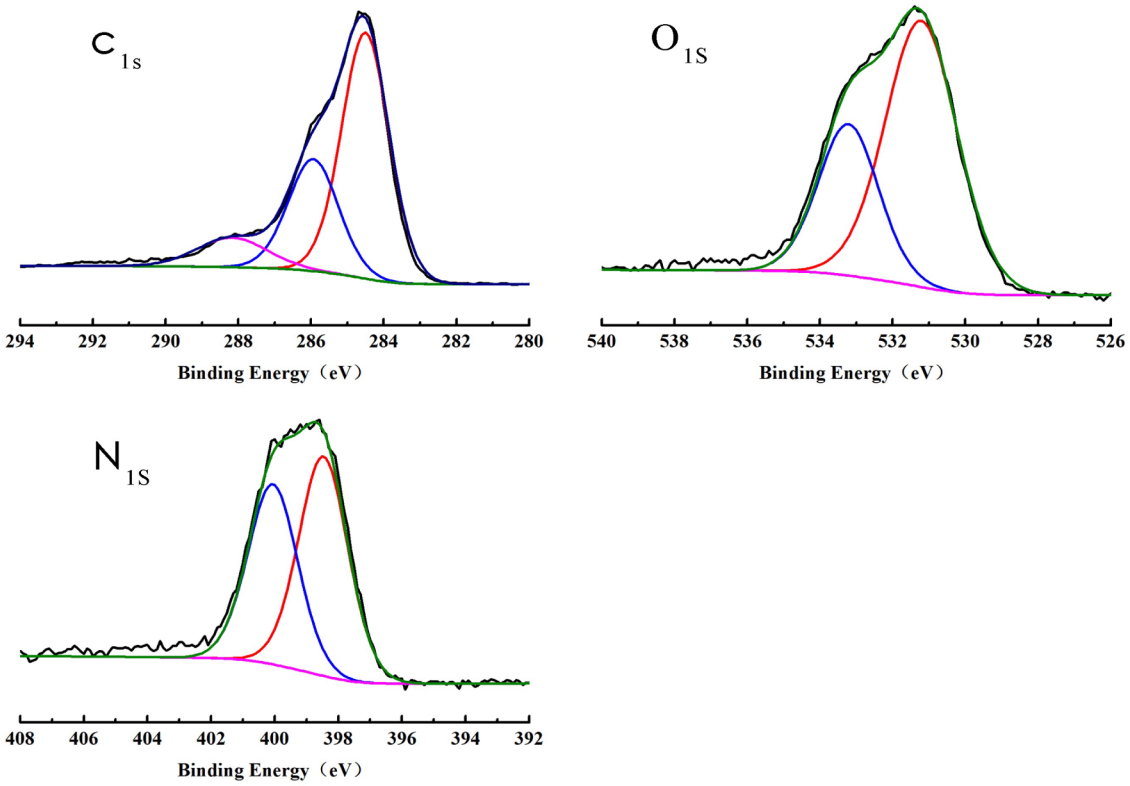

Figure 8. C 1s, O 1s, and N 1s XPS spectra of pure PU char residue.

listed in Table 4. From the tabulation, we can see that the $T_{-5\%}$ of pure PU is 277 °C, and its no char residue is 700 °C. The TGA curves show that with the increasing addition of FR, the char residue of material increases to 2.3% and the $T_{-5\%}$ temperature reduces to 262.9 °C. It is because the FR produces phosphoric acid and phosphorous acid during burning in the air. These substances have the strong capacity to dehydrate into carbon, increasing the material char residue material, which indicates that the phosphorus we synthesized achieves the purpose of flame retardancy through the mechanism of condensed-phase FR mechanism.

3.3. Analysis of PU Foam Surface Morphology of PU Foam Carbon Layer. As shown in Figure 7, the pure PU presents an evenly distributed flocculent structure. With the addition of FR, large pores and little carbon layers emerge in PU-5, distinct faults and cracks appear in PU-8, and a dense

https://doi.org/10.1021/acsomega.1c01267
ACS Omega 2021, 6, 16410−16418

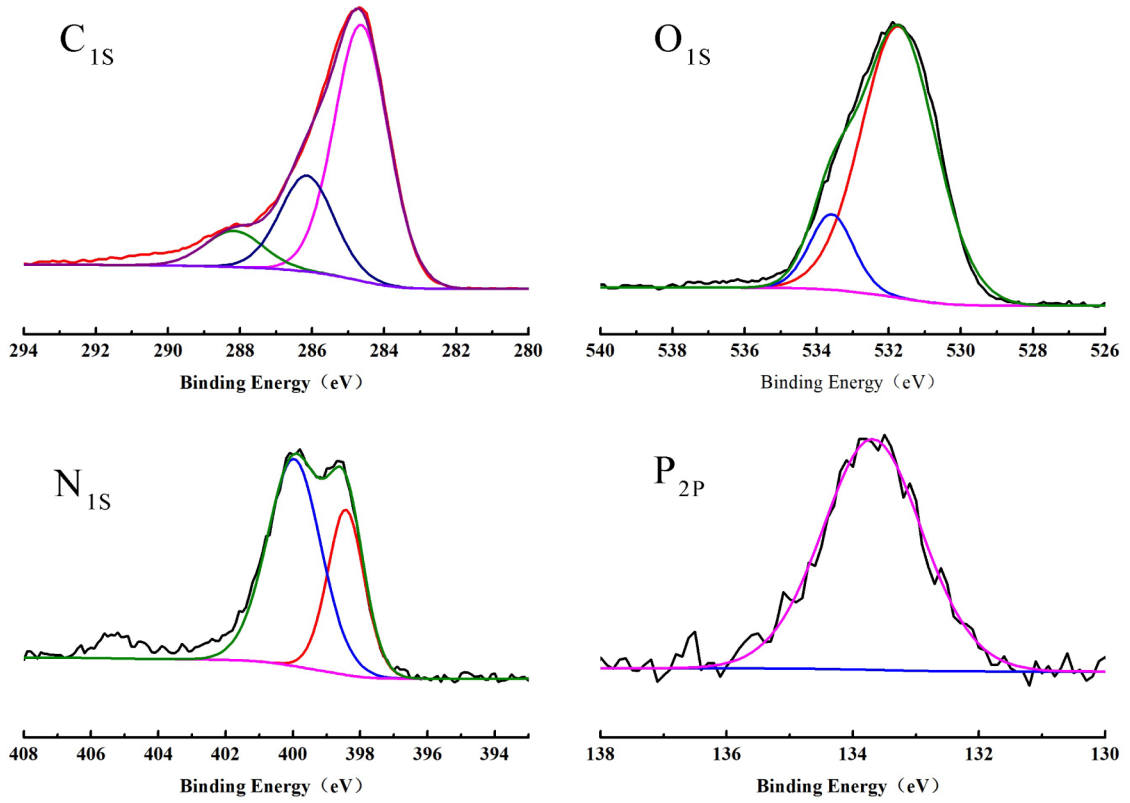

Figure 9. C 1s, O 1s, N 1s, and P 2p XPS spectra of PU-10 char residue.

carbon layer appears after combustion in PU-10. The different chars among samples are mainly because of the dehydration and carbonization of phosphoric acid during FR decomposition of phosphorus.[28] On one hand, the oxygen and heat were blocked by the char layers. On the other hand, the char payers can delay further combustion of the molten area.[29] Figure 7 (PU-10) shows that bubbles are uniformly distributed on the char layer, which may be because gas-phase FRs form volatile nitrogen elements (such as NO and NO_2) during the combustion process. For one thing, the volatilization of the nitrogen oxide absorbs lots of heat, and for another, nitrogen oxide reduces the concentration of oxygen.[30] According to the above results, HAMPP has both condensed-phase and gas-phase FR mechanisms. It means that HAMPP is an excellent P−N-containing FR in higher temperature that can promote the char residue.

3.4. Chemical Component Analysis of Char Residue at 500 °C. As shown in Figures 8 and 9, C 1s spectra has three bands: 284.6 eV peak attributes to C—H and C—C, 286.2 eV peak ascribes to C—O, and 288.2 eV peak assigns to C═O. By comparing the two sets of XPS data, the peak area of C—O decreases, while the C═O increases after adding HAMPP, which confirms that phosphorus-containing FR plays a strong dehydration role during combustion. O 1s spectra has two bands: the peak at 531.2 eV attributes to O═ and 533.2 eV peak belongs to the O—. Compared with the pure PU, the peak area belonging to O— abates and that belonging to O═ amplifies. This further shows that the P-containing cyclic in HAMPP forms a large number of phosphonate esters during combustion, indicating that HAMPP has a condensed-phase FR mechanism. The compound has a strong dehydration and carbonization effect on the matrix material. For the N 1s spectra, 398.5 eV is the peak of N—H, and 400.1 eV is the peak of nitrogen oxide. In Figure 9, the peak of nitrogen oxide becomes higher and the peak of N—H becomes lower. The peak at 400.1 eV can attribute to the formation of some nonflammable nitrogen oxides, such as nitric oxide and nitrogen dioxide during combustion. This result is consistent with the results of SEM. The single peak at 133.7 eV assigns to phosphonate and polyphosphate.[31−33]

3.5. Mechanical Property. From the mechanical performance data in Table 5, as small molecules, FRs can be used as chain extenders to increase the tensile strength and compressive strength of PU. The increase in elongation at break is due to the long alkyl chain structure in the FR. (Figures S7 and S8, respectively, show the tensile and compressive stress−strain curves.) It deduces that the FR is dispersed evenly in the material, and its addition does not cause phase separation, thereby increasing the strength of the material and also obviously improving the flexibility of the PU foam. From the mechanical performance data in Table 5, the tensile strength of PU-5 is the highest, which means that the less HAMPP added, the less impact on the material. HAMPP is dispersed well under the lower content of PU foam. The dihydroxy group can let the FR react into the main chain,

Table 5. Mechanical Property of Pure PU and PU-HAMPPs

samples	tensile strength (MPa)	elongation at break (%)	elastic modulus (MPa)	compressive strength (MPa)	compressive modulus (MPa)
pure-PU	0.31	138.99	0.48	0.49	0.7
PU-5	0.59	185.22	0.57	0.53	1.43
PU-8	0.46	199	0.35	0.89	1.27
PU-10	0.4	244.48	0.30	0.76	1.09

https://doi.org/10.1021/acsomega.1c01267
ACS Omega 2021, 6, 16410−16418

avoiding phase separation and providing a good dispersion basis.

4. CONCLUSIONS

In this paper, a reactive dihydroxy P−N-containing FR HAMPP was successfully developed. The flame retardancy performance of the HAMPP was evaluated with a series of HAMPPs-doped PU foams, which was prepared by copolymerizing HAMPP, polyether polyol, and diisocyanate. Our HAMPPs exhibited excellent flame retardancy and char layer ability to the flammable PU foam. The LOI value of PU-10 is up to 23.7%, which meets the V-0 rating (UL-94) requirement. By contrast to the PU foam without retardant, the PU-HAMPPs have a lower initial decomposition temperature and higher char residue. The FR decomposes at a lower temperature to form a dense char layer on the material surfaces and decomposes simultaneously to release NO and NO_2, which strongly indicated that the HAMPP exerts both elongation at break and the tensile strength of the material increased, indicating that the structure of the dihydroxy group in HAMPP helps the FR get better to integrate with the bulk material.

■ ASSOCIATED CONTENT

Supporting Information

The Supporting Information is available free of charge at https://pubs.acs.org/doi/10.1021/acsomega.1c01267.

^{1}H NMR of DMPP, HENE, and HAMPP; ^{31}P NMR of DMPP and HAMPP; the tensile and compressive stress−strain curves (PDF)

■ AUTHOR INFORMATION

Corresponding Author

Wenmu Li − *Key Laboratory of Optoelectronic Materials Chemistry and Physics, Fujian Institute of Research on the Structure of Matter, Chinese Academy of Sciences, Fuzhou 350002, China;* orcid.org/0000-0002-3481-5369; Email: liwm@fjirsm.ac.cn

Authors

Yulin Ding − *College of Chemistry and Material Science, Fujian Normal University, Fuzhou, Fujian 350007, China; Key Laboratory of Optoelectronic Materials Chemistry and Physics, Fujian Institute of Research on the Structure of Matter, Chinese Academy of Sciences, Fuzhou 350002, China*

Yumiao Su − *Key Laboratory of Optoelectronic Materials Chemistry and Physics, Fujian Institute of Research on the Structure of Matter, Chinese Academy of Sciences, Fuzhou 350002, China; University of Chinese Academy of Sciences, Beijing 100049, China*

Jiajing Huang − *College of Chemistry and Material Science, Fujian Normal University, Fuzhou, Fujian 350007, China; Key Laboratory of Optoelectronic Materials Chemistry and Physics, Fujian Institute of Research on the Structure of Matter, Chinese Academy of Sciences, Fuzhou 350002, China*

Ting Wang − *Key Laboratory of Optoelectronic Materials Chemistry and Physics, Fujian Institute of Research on the Structure of Matter, Chinese Academy of Sciences, Fuzhou 350002, China; University of Chinese Academy of Sciences, Beijing 100049, China*

Min-Yu Li − *College of Chemistry and Materials, Ningde Normal University, Ningde 352100, China*

Complete contact information is available at: https://pubs.acs.org/10.1021/acsomega.1c01267

Notes

The authors declare no competing financial interest.

■ ACKNOWLEDGMENTS

This work was supported by the Fujian STS plan supporting project (Project nos. 2019T3005 and 2019T3014), the High-Level Talents for Entrepreneurship and Innovation of Fujian Province, Young and Middle-aged Teacher Education Research Project of Fujian Provincial Department of Education (no. JT180604), and the Foundation of Ningde Normal University (no. 2018Q105).

■ REFERENCES

(1) Yang, H.; Yu, B.; Song, P.; Maluk, C.; Wang, H. Surface-coating engineering for flame retardant flexible polyurethane foams: A critical review. *Composites, Part B* **2019**, *176*, No. 107185.

(2) Chen, M.-J.; Shao, Z.-B.; Wang, X.-L.; Chen, L.; Wang, Y.-Z. Halogen-Free Flame-Retardant Flexible Polyurethane Foam with a Novel Nitrogen−Phosphorus Flame Retardant. *Ind. Eng. Chem. Res.* **2012**, *51*, 9769−9776.

(3) Pan, Y.; Liu, L.; Cai, W.; Hu, Y.; Jiang, S.; Zhao, H. Effect of layer-by-layer self-assembled sepiolite-based nanocoating on flame retardant and smoke suppressant properties of flexible polyurethane foam. *Appl. Clay Sci.* **2019**, *168*, 230−236.

(4) Su, Y.-M.; Wang, T.; Ding, Y.-L.; Huang, J.-J.; Li, W.-M. Preparation Technology of Solvent-free Polyurethane: A Mini-Review. *Chin. J. Struct. Chem.* **2020**, *39*, 2057−2067.

(5) Velencoso, M. M.; Battig, A.; Markwart, J. C.; Schartel, B.; Wurm, F. R. Molecular Firefighting-How Modern Phosphorus Chemistry Can Help Solve the Challenge of Flame Retardancy. *Angew. Chem., Int. Ed. Engl.* **2018**, *57*, 10450−10467.

(6) Alongi, J.; Carosio, F. Flame retardancy of flexible polyurethane foams. In *Novel Fire Retardant Polymers and Composite Materials*; Woodhead Publishing: 2017; pp 171−200.

(7) Wang, X.; Hu, Y.; Song, L.; Xing, W.; Lu, H.; Lv, P.; Jie, G. Flame retardancy and thermal degradation mechanism of epoxy resin composites based on a DOPO substituted organophosphorus oligomer. *Polymer* **2010**, *51*, 2435−2445.

(8) Zhao, H. B.; Wang, Y. Z. Design and Synthesis of PET-Based Copolyesters with Flame-Retardant and Antidripping Performance. *Macromol. Rapid Commun.* **2017**, *38*, 14.

(9) Stapleton, H. M.; Klosterhaus, S.; Keller, A.; Ferguson, P. L.; Van Bergen, S.; Cooper, E.; Webster, T. F.; Blum, A. Identification of flame retardants in polyurethane foam collected from baby products. *Environ. Sci. Technol.* **2011**, *45*, 5323−5331.

(10) Van Der Veen, I.; De Boer, J. Phosphorus flame retardants: Properties, production, environmental occurrence, toxicity and analysis. *Chemosphere* **2012**, *88*, 1119−1153.

(11) Brannum, D. J.; Price, E. J.; Villamil, D.; Kozawa, S.; Brannum, M.; Berry, C.; Semco, R.; Wnek, G. E. Flame-Retardant Polyurethane Foams: One-Pot, Bioinspired Silica Nanoparticle Coating. *ACS Appl. Polym. Mater.* **2019**, *1*, 2015−2022.

(12) Horacek, H.; Grabner, R. Advantages of flame retardants based on nitrogen compounds. *Polym. Degrad. Stab.* **1996**, *54*, 205−215.

(13) Ma, T.; Li, L.; Liu, T.; Guo, C. Synthesis of a caged bicyclic phosphates derived anhydride and its performance as a flame-retardant curing agent for epoxy resins. *Polym. Adv. Technol.* **2019**, *30*, 1314−1324.

(14) Liu, W.; Chen, L.; Wang, Y.-Z. A novel phosphorus-containing flame retardant for the formaldehyde-free treatment of cotton fabrics. *Polym. Degrad. Stab.* **2012**, *97*, 2487−2491.

(15) Kumar, N. S.; Kumaraswamy, S.; Said, M. A.; Swamy, K. C. K. Hydrolysis of cyclic phosphites/phosphoramidites and its inhibition-

reversible cyclization of acyclic phosphonate salts to cyclic phosphites. *Org. Process Res. Dev.* **2003**, *7*, 925−928.
(16) Duan, L.; Yang, H.; Song, L.; Hou, Y.; Wang, W.; Gui, Z.; Hu, Y. Hyperbranched phosphorus/nitrogen-containing polymer in combination with ammonium polyphosphate as a novel flame retardant system for polypropylene. *Polym. Degrad. Stab.* **2016**, *134*, 179−185.
(17) Xia, J.; Su, Y.; Li, W. Post-polymerization functionalization to a novel phosphorus- and nitrogen-containing polyether coating for flame retardant treatment of PET fabric. *J. Appl. Polym. Sci.* **2019**, *136*, No. 47299.
(18) Yu, Y.; Fu, S.; Song, P. A.; Luo, X.; Jin, Y.; Lu, F.; Wu, Q.; Ye, J. Functionalized lignin by grafting phosphorus-nitrogen improves the thermal stability and flame retardancy of polypropylene. *Polym. Degrad. Stab.* **2012**, *97*, 541−546.
(19) Nazir, R.; Gaan, S. Recent developments in P(O/S)−N containing flame retardants. *J. Appl. Polym. Sci.* **2019**, *137*, No. 47910.
(20) Liu, X.; Salmeia, K. A.; Rentsch, D.; Hao, J. W.; Gaan, S. Thermal decomposition and flammability of rigid PU foams containing some DOPO derivatives and other phosphorus compounds. *J. Anal. Appl. Pyrolysis* **2017**, *124*, 219−229.
(21) Yuan, Y.; Yang, H.; Yu, B.; Shi, Y.; Wang, W.; Song, L.; Hu, Y.; Zhang, Y. Phosphorus and Nitrogen-Containing Polyols: Synergistic Effect on the Thermal Property and Flame Retardancy of Rigid Polyurethane Foam Composites. *Ind. Eng. Chem. Res.* **2016**, *55*, 10813−10822.
(22) Wu, N.; Niu, F.; Lang, W.; Yu, J.; Fu, G. Synthesis of reactive phenylphosphoryl glycol ether oligomer and improved flame retardancy and mechanical property of modified rigid polyurethane foams. *Mater. Des.* **2019**, *181*, No. 107929.
(23) Wei, L.-L.; Wang, D.-Y.; Chen, H.-B.; Chen, L.; Wang, X.-L.; Wang, Y.-Z. Effect of a phosphorus-containing flame retardant on the thermal properties and ease of ignition of poly(lactic acid). *Polym. Degrad. Stab.* **2011**, *96*, 1557−1561.
(24) Chen, H. B.; Zhang, Y.; Chen, L.; Shao, Z. B.; Liu, Y.; Wang, Y. Z. Novel Inherently Flame-Retardant Poly(trimethylene Terephthalate) Copolyester with the Phosphorus-Containing Linking Pendent Group. *Ind. Eng. Chem. Res.* **2010**, *49*, 7052−7059.
(25) McConnell, R. L.; Coover, H. W. Phosphorus-Containing Derivatives of 2,2-Dimethyl-1,3-propanediol. *J. Org. Chem.* **1959**, *24*, 630−635.
(26) Wang, C.; Wu, Y.; Li, Y.; Shao, Q.; Yan, X.; Han, C.; Wang, Z.; Liu, Z.; Guo, Z. Flame-retardant rigid polyurethane foam with a phosphorus-nitrogen single intumescent flame retardant. *Polym. Adv. Technol.* **2018**, *29*, 668−676.
(27) Liu, L.; Wang, Z.; Zhu, M. Flame retardant, mechanical and thermal insulating properties of rigid polyurethane foam modified by nano zirconium amino-tris-(methylenephosphonate) and expandable graphite. *Polym. Degrad. Stab.* **2019**, *170*, No. 108997.
(28) Lin, H.-J.; Liu, S.-R.; Han, L.-J.; Wang, X.-M.; Bian, Y.-J.; Dong, L.-S. Effect of a phosphorus-containing oligomer on flame-retardant, rheological and mechanical properties of poly (lactic acid). *Polym. Degrad. Stab.* **2013**, *98*, 1389−1396.
(29) Lin, H.-J.; Han, L.-J.; Wang, X.-M.; Bian, Y.-J.; Li, Y.-S.; Dong, L.-S. Study on the thermal degradation behavior and flame-retardant property of polylactide/PEDPP blends. *Polym. Adv. Technol.* **2013**, *24*, 576−583.
(30) Shieh, J. Y.; Wang, C. S. Synthesis of novel flame retardant epoxy hardeners and properties of cured products. *Polymer* **2001**, *42*, 7617−7625.
(31) Yang, H.; Song, L.; Tai, Q.; Wang, X.; Yu, B.; Yuan, Y.; Hu, Y.; Yuen, R. K. K. Comparative study on the flame retarded efficiency of melamine phosphate, melamine phosphite and melamine hypophosphite on poly(butylene succinate) composites. *Polym. Degrad. Stab.* **2014**, *105*, 248−256.
(32) Xu, W. Z.; Liu, L.; Wang, S. Q.; Hu, Y. Synergistic effect of expandable graphite and aluminum hypophosphite on flame-retardant properties of rigid polyurethane foam. *J. Appl. Polym. Sci.* **2015**, *132*, 10.
(33) Huang, W.; He, W.; Long, L.; Yan, W.; He, M.; Qin, S.; Yu, J. Highly efficient flame-retardant glass-fiber-reinforced polyamide 6T system based on a novel DOPO-based derivative: Flame retardancy, thermal decomposition, and pyrolysis behavior. *Polym. Degrad. Stab.* **2018**, *148*, 26−41.

https://doi.org/10.1021/acsomega.1c01267
ACS Omega 2021, 6, 16410−16418